

# Small Craft Detection in Rough Seas

Stéphane Kemkemian, Myriam Nouvel, Vincent Corretja, Rodolphe Cottron, Ludovic Lupinski  
Thales Airborne Systems, France  
[stephane.kemkemian@fr.thalesgroup.com](mailto:stephane.kemkemian@fr.thalesgroup.com)

## Abstract:

*This paper deals with detection of small and slow targets in rough sea. After having summarized the statistical modelling of the sea clutter, the paper explains the interest of Track-Before-Detect (TBD) detectors for taking benefits of both high-resolution waveforms and sea clutter properties in the case of slow moving targets. Two affordable TBD detectors are compared to standard detectors working on a single dwell.*

**Keywords:** Maritime Radar, Sea Clutter, High Resolution Waveform, Track-Before-Detect.

## I. INTRODUCTION

The small craft detection ability in rough sea is of prime importance for maritime surveillance radars. On the one hand, regardless of the sea state, it is quite easy to detect fast moving targets by using Doppler filtering to isolate the thermal noise region from the clutter-contaminated region. On the other hand, in case of slow moving targets in high sea state, these targets remain embedded in sea clutter due to the intrinsic large spectral spreading of the sea clutter.

Indeed, the rougher the sea is, the wider the spectrum of sea clutter is. Fig. 1 illustrates this effect in up-wind conditions. Note that the intrinsic spectral width of sea clutter (not related to the motion of the radar platform) comes from the internal movements of the water mass.

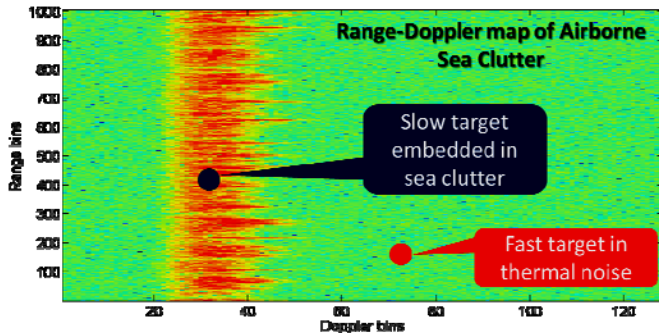


Fig. 1. Example of Distance-Doppler map of sea clutter

The slow targets are therefore to be detected from signal contaminated with sea clutter. The first possible way to improve detection is to reduce the geometric surface of resolution cells: this means using wideband waveforms. Another additional way is to reduce the mean reflectivity of the clutter by using observations at low grazing angle [1], [3]. Both methods aim to reduce the average clutter level. However, as much as the mean clutter is lowered, it turns to be very impulsive yielding high detection thresholds compared to the mean clutter + noise level [2]. For fully leveraging high-

resolution waveforms despite this, a “Track-Before-Detect” (TBD) processing is proposed.

The section II is dedicated to the description of some properties of sea clutter that are related to the proposed detection method. In section III, two affordable TBD processing are introduced. The optimisation of their parameters is described in IV.

## II. PROPERTIES OF SEA CLUTTER

With regard to the proposed method, the detection performance relies on two particular features of the sea clutter:

- The Probability Density Function (PDF) of its amplitude distribution yielding to the detection threshold at CFAR level;
- The Auto-Correlation Function (ACF) of clutter.

### 1 Amplitude distribution

It has been found [2], [3] that the sea clutter can be modelled by a compound random process in which the speckle  $x$  (locally Gaussian random process) is amplitude-modulated by an underlying mean intensity  $y$  or “texture” according to eqn. (1) where  $\sigma^2$  is the thermal noise power of receiver:

$$p(x|y, \sigma) = \frac{2x}{y + \sigma^2} \exp\left(-\frac{x^2}{y + \sigma^2}\right) \quad (1)$$

A correlated Gamma distribution (2) is often used to model the texture where  $\nu$  and  $b$  are respectively the shape and the scale parameter of the Gamma distribution:

$$p_c(y) = \frac{b^\nu}{\Gamma(\nu)} y^{\nu-1} \exp(-by) \quad (2)$$

The PDF of the interfering signal (clutter + noise) is thus:

$$p(x, \sigma) = \int_0^\infty p_c(y) p(x|y, \sigma) dy \quad (3)$$

In case of high Clutter-to-Noise Ratio (CNR), the noise can be neglected and the clutter amplitude follows a  $K$ -distribution with a closed form is given in eqn. (4) where  $K_\nu(\cdot)$  is the modified Bessel function of the  $\nu^{\text{th}}$  order:

$$p(x, 0) = \frac{4b^{(\nu+1)/2}}{\Gamma(\nu)} x^\nu K_{\nu-1}(2x\sqrt{b}) \quad (4)$$

The second order moment  $\langle x^2 \rangle = \mu = \nu/b$  is the mean power of clutter, thus  $CNR = \mu/\sigma^2$ . The Probability of False Alarm  $P_{FA}$  (*i.e.* the probability that an interfering signal exceeds a relative threshold  $\lambda_T$ ) is:

$$P_{FA} = \Pr\left(\frac{x^2}{\mu} > \lambda_T, \sigma\right) = \int_{\mu \lambda_T}^{+\infty} p(x^2) dx \quad (5)$$

If  $CNR \gg 1$ , the expression has a closed form:

$$P_{FA} = \Pr\left(\frac{x^2}{\mu} > \lambda_T, 0\right) = \frac{2(\nu \lambda_T)^{\frac{\nu}{2}}}{\Gamma(\nu)} K_{\nu}\left(2\sqrt{\nu \lambda_T}\right) \quad (6)$$

The mean power  $\mu$  can be related to the mean clutter R.C.S in a resolution cell:

$$\mu \propto \sigma^0 A \quad (7)$$

$A$  is the geometric surface of a resolution cell (depending on the waveform) and  $\sigma^0$  is the mean clutter reflectivity.  $A$  is related to the range resolution  $\delta r$ :

$$A \approx 0.75 R \theta_{AZ} \delta r \quad (8)$$

$R$  is the distance and  $\theta_{AZ}$  is the beam width.

The shape parameter  $\nu$  is also depending on the surface  $A$  and the geometry of observation. An empirical model is given in eqn. (9) ( $\varepsilon$  is the grazing angle in degrees and  $\varphi$  is the angle between the antenna beam and the swell direction).  $k_{POL}$  is equal to 2.09 in HH polarization and 1.39 in VV polarization [3]:

$$\log_{10}(\nu) = \frac{2}{3} \log_{10}(\varepsilon) + \frac{5}{8} \log_{10}(A) - \frac{\cos(2\varphi)}{3} - k_{POL} \quad (9)$$

In the case where no swell is present, the third term is zero.

### 2 Detection capability on a single dwell (one antenna turn)

The  $P_{FA}$  as function of the Non-Normalized Threshold  $\lambda_{NNT} = \mu \lambda_T = \sigma^0 A \lambda_T$  is presented in Fig. 2 for three range resolutions (1m, 10m and 100m) the same cross-range resolution  $L \approx 0.75 R \theta_{AZ} = 1000m$  and  $\sigma^0 = -40dB$ . These curves are valid for  $CNR \gg 1$ .

Depending on the  $P_{FA}$ , the value of this threshold yields an estimation of the minimum detectable target R.C.S. (necessary but not sufficient condition, one other necessary condition being a sufficient Signal-to-Noise-Ratio SNR). Indeed, a target echo having a power equal to the threshold corresponds to a probability of detection of about 30%.

The solid curves are related to K-distributed clutter ( $\nu$  set from eqn. (9)) whereas the dotted curves are related to Gaussian clutter ( $\nu = \infty$ ). These simulations lead to the following conclusions:

- In the case of Gaussian clutter, the detection threshold is directly proportional to the range resolution. There is therefore a clear interest in reducing  $\delta r$  as long as the target size remains small with respect to this range resolution.
- In the case of K-distributed clutter (or also with other long-tailed PDF), it should be noted several effects:
  - When working with low  $P_{FA}$  (e.g.  $< 10^{-5}$ ), little improvement is gained by reducing  $\delta r$ . In

addition, there is a very large threshold difference between the K case and the Gaussian case.

- However, by working at much higher PFA (e.g.  $10^{-2}$ ), the behaviour becomes similar to the Gaussian case's behaviour.

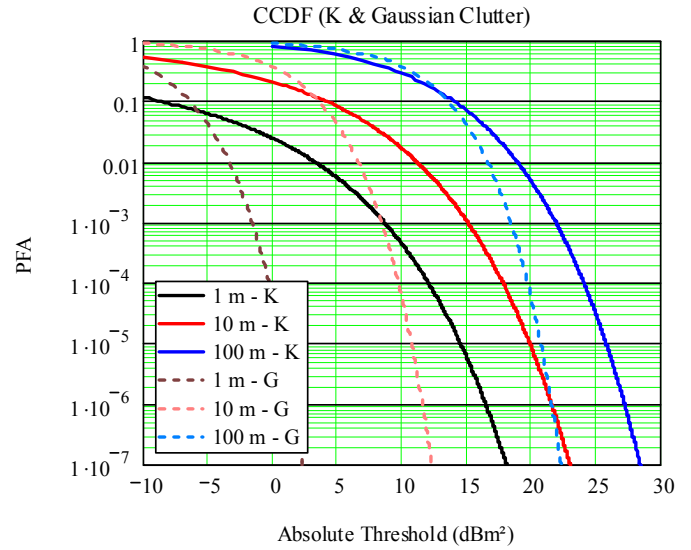


Fig. 2. Probability of false alarm as function of the Non-Normalized Threshold (one single pulse). Solid curves: K-distributed clutter, dotted curves: Gaussian clutter.

The proposed solution is therefore a post-processing running over several antenna revolutions that allows working with high PFA at first thresholding. An enabler to perform this in the case of sea clutter is its correlation properties.

### 3 Correlation Properties of Sea Clutter

The Auto-Correlation Function (ACF) of the underlying intensity  $y$  lasts greater than a dwell time [5].

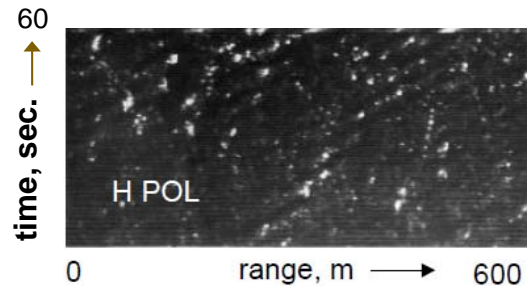


Fig. 3. Mean intensity of sea clutter

The property of sea clutter, which is taken advantage here, is that the texture  $y$  can be assumed independent from one antenna turn to other antenna turn. This is because the sea surface is a deformable surface (which is fundamentally different from ground clutter). This property is illustrated in Fig. 3 showing a high-resolution range profile of sea clutter observed during a few tens of seconds with a starring antenna.

### III. TRACK-BEFORE-DETECT DETECTORS

#### 1 Principle of TBD detectors

The TBD performs the detection process in two steps:

- **First step** (during each antenna revolution): Pre-detection using low CFAR threshold (*i.e.* yielding high  $P_{FA}$ ). The small targets as well as many false alarms pass this test.
- **Second step** (from one antenna turn to another one): A test based on a kinematic model allows rejecting false alarms while keeping the targets' detections.

These detectors operate on a moving window of  $N \geq 2$  antenna revolutions. The general principle of TBD detectors is to extract, on a moving window of  $N$  antenna revolutions, sets of successive pre-detections  $\mathbf{S}^j = \{s_1^j, \dots, s_m^j\}$  that fulfil a given kinematic model. The cardinality of such a set verify  $2 \leq m(j) = \text{card}(\mathbf{S}^j) \leq N$ . A set of pre-detection  $\mathbf{S}^j$  indicates a validated target if:

$$\text{card}(\mathbf{S}^j) \geq K \quad (10)$$

The parameter  $K$  being the second detection threshold.

#### 2 Affordable TBD detectors

At first glance, one could imagine carrying out the kinematic tests using traditional tracking filters such as Kalman filters with suitable target model. However, the use of high-resolution waveforms results in a very large number of resolution cells examined at each antenna revolution (order of  $10^6$  to  $10^7$ ). The goal of the TBD is to achieve working with a very high  $P_{FA}$  at the first threshold (about  $10^{-2}$  even more). In these conditions, about  $10^4$  to  $10^5$  new Kalman filters should be open at each antenna revolution. This is quite intractable with affordable real time data processors. That is why another approach to the implementation of the kinematic tests is proposed in this paper.

Two kinematic models are well suited to the detection of slow moving targets even fixed targets: the fixed target model (FTM) and the constant velocity model (CVM). First, we are going to determine the reference performance on a single dwell without any TBD processing.

#### 3 Detection performance without TBD

Suppose that the operational requirement is “no more than  $N_{FA}$  false detection(s) per antenna turn”. During one antenna revolution the number of resolution cells, where the detection test is performed, is given by:

$$N_{CELL} = \frac{2\pi R_{MAX}}{\theta_{AZ} \delta r} \Rightarrow \quad (11)$$

$$P_{FA\_CFAR\_0} \cong \frac{N_{FA}}{N_{CELL}} = N_{FA} \frac{\theta_{AZ} \delta r}{2\pi R_{MAX}}$$

Table 1. *PFA and non-normalized threshold*

( $R_{MAX} = 100$  km,  $\theta_{AZ} = 50$  mrd,  $N_{FA} = 1$  and  $\sigma^0 = -40$  dB)

$\delta r$	100 m	10 m	1 m
$N_{CELL}$	$1.25 \cdot 10^5$	$1.25 \cdot 10^6$	$1.25 \cdot 10^7$
$P_{FA\_CFAR\_0}$	$8 \cdot 10^{-6}$	$8 \cdot 10^{-7}$	$8 \cdot 10^{-8}$
$\lambda_{NNT}$	<b>26 dBm<sup>2</sup></b>	<b>22 dBm<sup>2</sup></b>	<b>18 dBm<sup>2</sup></b>

The values of  $P_{FA\_CFAR}$  and  $\lambda_{NNT}$  are reported in Fig. 4 (“Single dwell detection”):

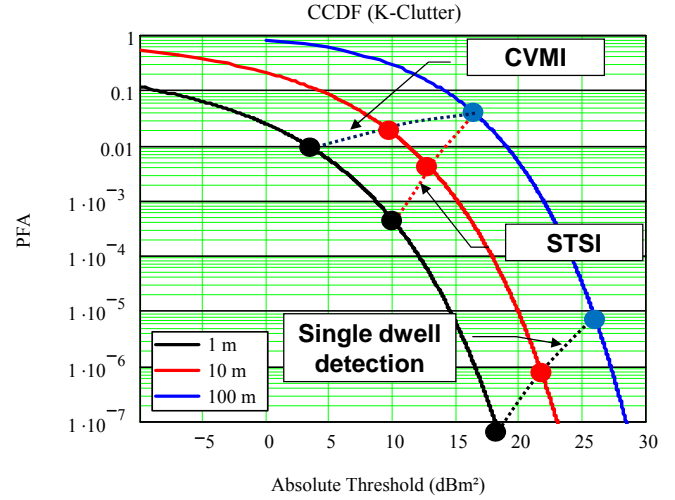


Fig. 4. *Probability of false alarm as function of non-normalized threshold  $\lambda_{NNT}$  (one single pulse).*

#### 4 Scan-To-Scan Integrator (STSI)

##### 1) Principle:

The kinematic model of this detector is the stationary target. Its implementation consists in using a memory in which each correlation bin corresponds to a small Distance-Azimuth domain (but containing several resolution cells). At each antenna revolution, the pre-detections (1<sup>st</sup> detection step) are reported in the nearest Range-Azimuth memory bin. After  $N$  antenna's revolutions, the bins where the pre-detection score is  $\geq K$  ( $K$  out of  $N$  criterion, cf. eqn. (10)) are confirmed targets (second detection step) [6]. The bins' dimensions are determined as follows: if  $\Delta V$  is the maximum target's velocity (kinematic model),  $T$  is the rotation period of antenna,  $\sigma_R$  and  $\sigma_{AZ}$  are respectively the standard deviations of the range and azimuth measurements, the bin dimensions are:

$$\begin{aligned} \Delta R &= N \Delta V T + \alpha \sigma_R \\ \Delta Az &= N \Delta V T / R + \alpha \sigma_{Az} \end{aligned} \quad (12)$$

The coefficient  $\alpha$  is chosen so that the probability of a greater position error  $\alpha \sigma$  due to the measurement noise is negligible ( $\alpha \approx 3$ ). For example if  $NT\Delta V = 180$ m,  $R = 50$ km,  $\sigma_R = 10$ m,  $\sigma_{Az} = 10$ mrd:

$$\Delta R = 180\text{m} + 30\text{m} = 210\text{m}$$

$$\Delta Az = 3.6\text{mrd} + 30\text{mrd} = 33.6\text{mrd}$$

In other words, the bin size is driven by the maximum target motion in range and driven by the angle accuracy in azimuth.

## 2) False alarm rate at pre-detection level

Using the same operational requirement as in subsection 3, the number of correlation bins within the detection domain ( $R_{MAX}, 2\pi$ ) and the  $P_{FA}$  per bin is:

$$N_{BIN} = \frac{2\pi R_{MAX}}{\Delta R \Delta A_z} \Rightarrow \quad (13)$$

$$P_{FA\_STS} \cong \frac{N_{FA}}{N_{BIN}} = N_{FA} \frac{\Delta R \Delta A_z}{2\pi R_{MAX}}$$

This value corresponds to the  $P_{FA}$  at the output of the STSI. Assuming that the false alarms are independent between successive revolutions (fundamental hypothesis about sea clutter, cf. subsection III.3), the  $P_{FA}$  before the STSI within a correlation bin can be determined using the binomial formula:

$$P_{FA\_STS} = \sum_{i=K}^N \binom{N}{i} P_{FA\_BIN}^i (1 - P_{FA\_BIN})^{N-i} \quad (14)$$

$$P_{FA\_STS} \cong \binom{N}{K} P_{FA\_BIN}^K$$

The number of resolutions cells in a correlation bin and the required  $P_{FA}$  at the level of the resolution cell are:

$$n = \frac{\Delta R \Delta A_z}{\theta_{AZ} \delta r} \geq 1 \quad P_{FA\_CFAR\_1} \cong \frac{P_{FA\_BIN}}{n} \quad (15)$$

Eqns. (14) and (15) are valid if  $P_{FA\_BIN} \ll 1$  otherwise exact calculation is required. Merging (13), (14) and (15), yields:

$$P_{FA\_CFAR\_1} \cong \frac{\theta_{AZ} \delta r}{\Delta R \Delta A_z} \left( \frac{1}{\binom{N}{K}} N_{FA} \frac{\Delta R \Delta A_z}{2\pi R_{MAX}} \right)^{\frac{1}{K}} \quad (16)$$

Comparing eqns. (11) and (16), the ratio of  $P_{FA}$  with STSI and w/o STSI is then:

$$\frac{P_{FA\_CFAR\_1}}{P_{FA\_CFAR\_0}} \approx \left( \frac{1}{\binom{N}{K}} \right)^{\frac{1}{K}} \left( \frac{1}{N_{FA}} \times \frac{2\pi R_{MAX}}{\Delta R \Delta A_z} \right)^{\frac{K-1}{K}} \quad (17)$$

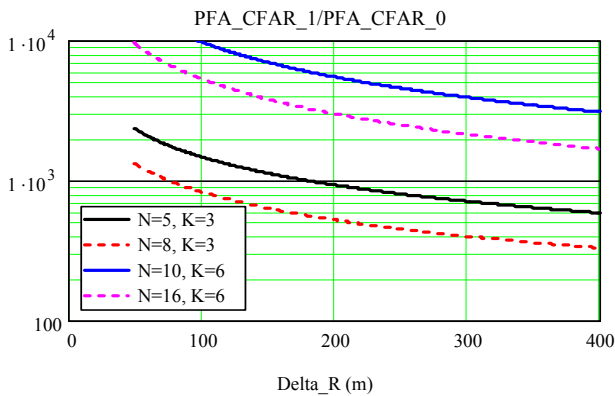


Fig. 5. Increase of  $P_{FA}$  par resolution cell due to STSI processing.  $N_{FA}=1$ ,  $\Delta A_z = 35\text{mrd}$  and  $R_{MAX} = 100\text{km}$ .

This ratio does not depend on waveform resolution and it is illustrated in Fig. 5. For instance ( $N = 10$ ,  $K = 6$  and  $\Delta R = 200\text{m}$ ) allows operating with a  $P_{FA}$  increased by a factor of 5500 compared to the direct detection. The table 1 becomes:

Table 2.  $P_{FA}$  and non-normalized threshold

$\delta r$	100 m	10 m	1 m
$N_{CELL}$	$1.25 \cdot 10^5$	$1.25 \cdot 10^6$	$1.25 \cdot 10^7$
$P_{FA\_CFAR\_0}$	$8 \cdot 10^{-6}$	$8 \cdot 10^{-7}$	$8 \cdot 10^{-8}$
$\lambda_{NNT}$ (w/o STSI)	<b>26 dBm<sup>2</sup></b>	<b>22 dBm<sup>2</sup></b>	<b>18 dBm<sup>2</sup></b>
$P_{FA\_CFAR\_1}$	$4.4 \cdot 10^{-2}$	$4.4 \cdot 10^{-3}$	$4.4 \cdot 10^{-4}$
$\lambda_{NNT}$ (with STSI)	<b>16 dBm<sup>2</sup></b>	<b>12 dBm<sup>2</sup></b>	<b>10 dBm<sup>2</sup></b>

On the one hand, the smaller the dimensions ( $\Delta R, \Delta A_z$ ) of the correlation cells are, the lower the detection threshold is. On the other hand, the maximum velocity  $\Delta V$  of targets is limited (cf. eqn. (12)). The kinematic criterion described at next subsection mitigates this drawback.

## 5 CVM Integrator

The target model used in STSI makes no hypothesis on the target trajectory within a correlation bin. For instance, a random walk where the target remains within the correlation bin fulfils the criterion (Fig. 6).

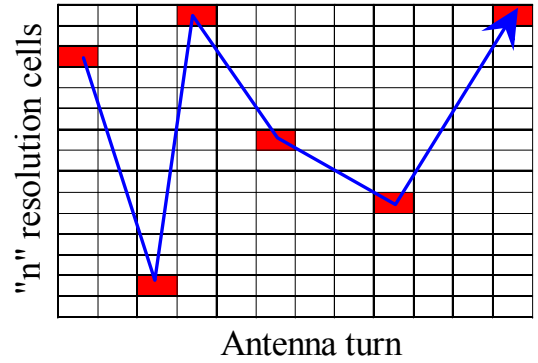


Fig. 6. Random walk fulfilling the STSI criterion

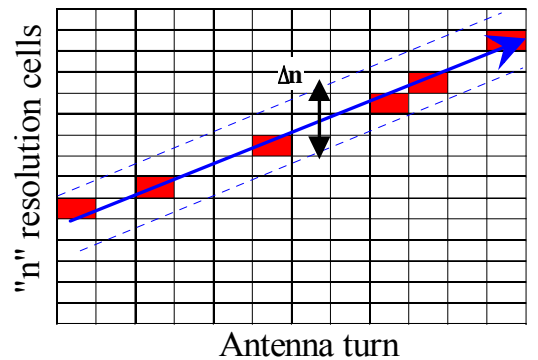


Fig. 7. Trajectory fulfilling the CVM.

A more selective criterion is to check the alignment of successive pre-detections (Constant Velocity Model). A possible method consist in applying a least square fit to the

range-azimuth measurements (assuming that  $\Delta R \ll R$  and  $\Delta z \ll 1$ ). A pre-detection set  $S^j$  having passed the STSI test is finally validated if the mean quadratic error is under a given threshold (Fig. 7). This later test requires that  $K \geq 3$ . This additional kinematic test allows working with an increased  $P_{FA\_CFAR}$  or conversely a decreased threshold. It can be demonstrated that [6]:

$$\frac{P_{FA\_CFAR\_2}}{P_{FA\_CFAR\_1}} \approx \left(\frac{n}{\Delta n}\right)^{\frac{K-2}{K}} \quad (18)$$

For instance, for the same numerical example used for tables 1 and 2, we get now:

Table 3.  $P_{FA}$  and non-normalized threshold

$\delta r$	100 m	10 m	1 m
$N_{CELL}$	$1.25 \cdot 10^5$	$1.25 \cdot 10^6$	$1.25 \cdot 10^7$
$P_{FA\_CFAR\_0}$	$8 \cdot 10^{-6}$	$8 \cdot 10^{-7}$	$8 \cdot 10^{-8}$
$\lambda_{NNT}$ (w/o STSI)	<b>26 dBm<sup>2</sup></b>	<b>22 dBm<sup>2</sup></b>	<b>18 dBm<sup>2</sup></b>
$P_{FA\_CFAR\_1}$	$4.4 \cdot 10^{-2}$	$4.4 \cdot 10^{-3}$	$4.4 \cdot 10^{-4}$
$\lambda_{NNT}$ (with STSI)	<b>16 dBm<sup>2</sup></b>	<b>12 dBm<sup>2</sup></b>	<b>10 dBm<sup>2</sup></b>
$n/\Delta n$	1	10	100
$P_{FA\_CFAR\_2}$	$4.4 \cdot 10^{-2}$	$2.0 \cdot 10^{-2}$	$9.5 \cdot 10^{-3}$
$\lambda_{NNT}$ (with CVMI)	<b>16 dBm<sup>2</sup></b>	<b>10 dBm<sup>2</sup></b>	<b>3 dBm<sup>2</sup></b>

This table shows the effectiveness of a TBD processing when used with a high-resolution waveform on impulsive clutter.

#### IV. OPTIMUM “K OUT OF N” CRITERIONS

The number of turns  $N$  is limited by the maximum delay to declare detection (operational requirement). For given  $CNR$ ,  $SNR$ ,  $N_{FA}$ , waveform parameters, clutter conditions and kind of TBD, the CFAR detection threshold  $\lambda_T$  is finally a function of  $K$ .

On the one hand, the higher the value of  $K$  is, the lower the detection threshold is, and the easier a target can exceed  $\lambda_T$  (single dwell). On the other hand, the higher the value of  $K$  is, the more difficult for a target to pass the “ $K$  out of  $N$ ” test is. The probability to detect a Swerling 1 target on sea surface with a single dwell is given in eqn. (19) (only one pulse):

$$P_D(S_T, K) = \exp\left(-\frac{\lambda_T(K)}{1+S_T}\right) \quad (19)$$

The probability of detection after the “ $K$  out of  $N$ ” test is then given by the binomial formula:

$$P_{D\_STSI}(S_T, K) = \sum_{i=K}^N \binom{N}{i} P_D^i(S_T, K) [1 - P_D(S_T, K)]^{N-i} \quad (20)$$

The curves in Fig. 8 are plotted by merging eqns. (18) and (19). Given  $N$  and  $N_{FA}$ , there is a value  $K$  that maximizes the probability of detection. Nevertheless, numerical simulations are necessary to assess the optimum.

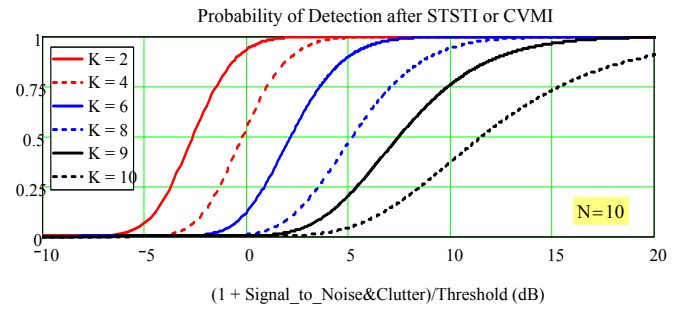


Fig. 8. Probability of detection at the output of STSI or CVMI as function of the relative target level.

#### V. CONCLUSION

This paper highlights the value of using detection processing on multiple antenna revolutions (Track-Before-Detect) to take benefit of the correlation properties of sea clutter. To take advantage of these properties, a wide-bandwidth waveform is required. Two affordable types of TBD processing for real time operation are presented and compared.

#### REFERENCES

- [1] M. M. Horst, F. B. Dyer and M. T. Tuley, “Radar Sea Clutter Model,” *IEEE International Conference on Antennas and Propagation*, Part 2, 1978.
- [2] S. Watts, “Radar detection prediction in sea clutter using the compound K-distribution model”, *IEE Proc. F-Commun., Radar Signal Process.*, 1985, 132, (7), pp. 613–620.
- [3] S. Watts, “Radar Sea Clutter Modelling – Recent Progress and Future Challenges,” *International Conference Radar 08*, Adelaide, September 2008.
- [4] S. Watts, “A new method for the simulation of coherent radar sea clutter,” 2011 IEEE Radar Conference RadarCon ‘11, Kansas City, May 2011, paper 3033.
- [5] S. Watts, “Modeling and simulation of coherent sea clutter,” *IEEE Trans AES Vol. 48, No.4, October 2012*, pp. 3303-3317.
- [6] S. Kemkemian and J.-M. Queller, “Détection de navires par radars maritimes - Signaux et traitements”, *les Techniques de l’Ingénieur - RAD6709*, 10 february 2014.

#### BIO DATA OF AUTHORS



**Stéphane Kemkemian** is Senior Radar Expert within the Technical Directorate at THALES Airborne Systems. He is Design Authority in several surveillance programs. He graduated in Aerospace Engineering from ISAE, France.

**Myriam Nouvel** is Head of Technical Simulation within the Technical Directorate at THALES Airborne Systems. She is Ph.D. in signal processing.

**Vincent Corretja** is study Engineer within THALES Airborne Systems. He is Ph.D. in signal processing.

**Rodolphe Cotttron** is Radar Expert within THALES Airborne Systems.

**Ludovic Lupinski** is Senior Radar Expert within the Technical Directorate at THALES Airborne Systems.